01 Aug 2012

Gallium Containing Glass Polyalkenoate Anti-Cancerous Bone Cements: Glass Characterization and Physical Properties

A. W. Wren

A. Coughlan

L. Placek

Mark R. Towler
Missouri University of Science and Technology, mtowler@mst.edu

Recommended Citation

A. W. Wren et al., "Gallium Containing Glass Polyalkenoate Anti-Cancerous Bone Cements: Glass Characterization and Physical Properties," *Journal of Materials Science: Materials in Medicine*, vol. 23, no. 8, pp. 1823 - 1833, Springer, Aug 2012.
The definitive version is available at https://doi.org/10.1007/s10856-012-4624-4

J Mater Sci: Mater Med (2012) 23:1823–1833
DOI 10.1007/s10856-012-4624-4

Gallium containing glass polyalkenoate anti-cancerous bone cements: glass characterization and physical properties

A. W. Wren · A. Coughlan · L. Placek · M. R. Towler

Received: 31 August 2011 / Accepted: 17 March 2012 / Published online: 9 June 2012

Abstract A gallium (Ga) glass series ($0.48SiO_2$–0.40ZnO–0.12CaO, with 0.08 mol% substitution for ZnO) was developed to formulate a Ga-containing Glass Polyalkenoate Cement (GPC) series. Network connectivity (NC) and X-ray Photoelectron Spectroscopy (XPS) was employed to investigate the role of Ga^{3+} in the glass, where it is assumed to act as a network modifier. Ga-GPC series was formulated with E9 and E11 polyacrylic acid (PAA) at 50, 55 and 60 wt% additions. E11 working times (T_w) ranged from 68 to 96 s (*Lcon.*) and 106 s for the Ga-GPCs (*LGa-1* and *LGa-2*). Setting times (T_s) ranged from 104 to 226 s (*Lcon.*) and 211 s for *LGa-1* and *LGa-2*. Compression (σc) and biaxial flexural (σf) testing were conducted where *Lcon.* increased from 62 to 68 MPa, *LGa-1* from 14 to 42 MPa and *LGa-2* from 20 to 47 MPa in σc over 1–30 days. σf testing revealed that *Lcon.* increased from 29 to 42 MPa, *LGa-1* from 7 to 32 MPa and *LGa-2* from 12 to 36 MPa over 1–30 days.

1 Introduction

Bioactive glasses have been of interest in recent years in the development of biomaterials for bone tissue engineering. Pioneering the field of bioactive glasses was L. Hench with the development of Bioglass, a SiO_2–CaO–Na_2O–P_2O_5 based glass which, at a specific composition, is known to bond directly to bone and soft tissues [1, 2]. The therapeutic effect of these materials is due to the ion dissolution from the glass in vivo, thus stimulating a cellular response which encourages bone ingrowth [2–4]. Bioactive glasses of varying composition have since been used in numerous forms as bone augmenting materials, in particular as composite materials due to the therapeutic nature of the glass. They have been included in PMMA based bone cements to enhance the bioactive response [5, 6]. They have also been coated on the surface of metallic implants such as hip stems, to induce a more stable bond between the host tissue and the implant [7]. Bioglass in particular has been coated on many polymers (polyurethane) [8]/ biopolymers (collagen, chitin, chitosan, silk) [9] in order to produce scaffolds for cell seeding which enhances their biological response [9–16].

Bioactive glasses can be one of the major components of Glass Polyalkenoate Cements (GPCs) which are traditionally dental materials used for restorative purposes such as filling cavities in teeth, lining and luting applications [17, 18]. These materials set by an acid base reaction between a polyalkenoic acid (polyacrylic acid—PAA) and an acid degradable glass which is conventionally an alumino-silicate based glass [17, 19, 20]. The glass phase generally comprises a SiO_2–CaO–Al_2O_3 or SiO_2–CaF–Al_2O_3 glass which may also contain varying concentrations of sodium (Na), lanthanum (La), strontium (Sr), fluorine (F) and phosphorus (P) depending on the GPC [18, 21]. These materials have been widely used in dentistry due to their suitable mechanical properties and their antibacterial nature (imparted by F^- release) which prevents secondary caries formation [22–24]. They also lack any significant shrinkage upon setting and have a low curing temperature [25]. Another attractive feature of these materials is that they can be modified to tailor their properties by either altering the molecular weight of the PAA used or by changing the composition of the glass phase.

A. W. Wren (✉) · A. Coughlan · L. Placek · M. R. Towler
Inamori School of Engineering, Alfred University, Alfred, NY 14802, USA
e-mail: wren@alfred.edu

Research has expanded from using these materials in dentistry to modifying them for orthopaedic applications. One of the most important changes in the transition of these materials from dental to orthopaedics is changing the glass composition to incorporate ions that have a positive therapeutic effect on bone (Sr^{2+}, Zn^{2+}, Ca^{2+}), and in particular to remove aluminium (Al^{3+}) which is known to deleteriously influence bone metabolism [26] and has also been implicated in numerous neurological disorders [27, 28]. Previous work by the authors has seen the development of a SiO_2–CaO–SrO–ZnO based GPC series for orthopaedics, in particular for stabilization of osteoporotic vertebral augmentation such as Vertebroplasty and Kyphoplasty [29–32]. Some properties of these materials, including mechanical and rheological properties and bioactivity were further improved by subsequently substituting titanium (Ti) for the silica content within the glass phase [33–35].

The focus of this work is to develop a series of GPCs that contain gallium (Ga) which is known to have a therapeutic effect in treating bone cancer [36]. Radioactive gallium and stable gallium nitrate are used as diagnostic and therapeutic agents in cancer and disorder of calcium and bone metabolism [37]. Gallium compounds have also shown anti-inflammatory and immunosuppressive activity in animal models of human disease [37]. Other reported studies show that the administration of between 30 and 60 mg/kg/24 h over a 10 days period in mice that had a solid tumor sub-cutaneously transplanted, inhibited tumour growth by more than 90 % in six out of the eight experimental rodents [38].

This work sees the development of a Ga-containing GPC that can be injected into cavities created in bone post-surgical resection of a tumorous growth. Ga release from these cements may eradicate any remaining cancerous cells preventing further growth and proliferation thus providing an important therapeutic effect while also filling the cavity created by the surgical procedure.

2 Materials and methods

2.1 Glass synthesis

Three Ga containing glass compositions (*Lcon., LGa-1, LGa-2*) were formulated for this study with the principal aim being to investigate and property changes with the addition of Ga to a cement. The control glass was a Ga-free CaO–ZnO–SiO_2 glass, *LGa-1* and *LGa-2* contain incremental concentrations of Ga at the expense of zinc (Zn). Glasses were prepared by weighing out appropriate amounts of analytical grade reagents (Sigma–Aldrich, Dublin, Ireland) and ball milling (1 h). The mix was then oven dried (100 °C, 1 h) and fired (1,500 °C, 1 h) in a platinum crucible and shock quenched into water. The resulting frit was dried, ground and sieved to retrieve a glass powder with a maximum particle size of 45 μm (Table 1).

Table 1 Glass compositions (mol%)

	Control	LGa-1	LGa-2
SiO_2	0.48	0.48	0.48
Ga_2O_3	0.00	0.08	0.16
ZnO	0.40	0.32	0.24
CaO	0.12	0.12	0.12

2.2 Glass characterisation

2.2.1 X-ray diffraction (XRD)

Diffraction patterns were collected using a Siemens D5000 X-ray Diffraction Unit (Bruker AXS Inc., WI, USA). Glass powder samples were packed into standard stainless steel sample holders. A generator voltage of 40 kV and a tube current of 30 mA was employed. Diffractograms were collected in the range $10° < 2\theta < 80°$, at a scan step size 0.02° and a step time of 10 s. Any crystalline phases present were identified using JCPDS (Joint Committee for Powder Diffraction Studies) standard diffraction patterns.

2.2.2 Differential thermal analysis (DTA)

A combined differential thermal analyser-thermal gravimetric analyser (DTA-TGA) (SDT 2960 Simultaneous DSC-TGA, TA Instruments, DW, USA) was used to measure the glass transition temperature (T_g) for both glasses. A heating rate of 20 °C min^{-1} was employed using an air atmosphere with alumina in a matched platinum crucible as a reference. Sample measurements were carried out every 6 s between 30 and 1,300 °C.

2.2.3 Network connectivity (NC)

The network connectivity (NC) of the glasses was calculated with Eq. 1 using the molar compositions of the glass. Network connectivity calculations were performed assuming that Ti performs as a network former and also as a network modifier.

$$\mathrm{NC} = \frac{\text{No. BOs} - \text{No. NBOs}}{\text{Total No. Bridging Species}} \quad (1)$$

where NC = Network Connectivity, BO = Bridging Oxygens, NBO = Non-Bridging Oxygens.

2.2.4 X-ray photoelectron spectroscopy (XPS)

X-ray Photoelectron Spectroscopy (XPS) was performed using a PHI Quantera SXM Scanning X-ray Microprobe to analyze the surface chemistry, as well as the chemical state of the top few nanometers of the samples. Survey scans were used to monitor the presence of any contaminants. The Analytical parameters include a 100 μm spot size, 25 W, 15 kV, 240 eV pass energy, 0.5 eV step size, 3 sweeps, and a binding energy range of 0–1,100 eV. High resolution scans were then acquired of the binding energy regions associated with the each element present in the glass. Spot size, power, and voltage were held consistent, however the pass energy and step size was reduced to 55 and 0.05 eV respectively, and the number of sweeps was raised to 5. All data was normalized based on the C1 s peak position of 284.8 eV.

2.3 Sample preparation

Cements were prepared by thoroughly mixing the glass powders (<45 μm) with E9 and E11 polyacrylic acid (PAA–M*w*, 80,800 and 210,000, <90 μm, Advanced Healthcare Limited, Kent, UK) and distilled water on a glass plate. The cements were formulated in a P:L ratio of 2:1.5 with 50, 55 and 60 wt% additions of PAA in order to determine the material with the most suitable handling and mechanical properties. Complete mixing was undertaken within 20 s.

2.4 Working and setting times

The setting times (T_s) of the cement series were tested in accordance with ISO9917 which specifies the standard for dental water based cements [39]. The working time (T_w) of the cements was measured in ambient air using a stopwatch, and was defined as the period of time from the start of mixing during which it was possible to manipulate the material without having an adverse effect on its properties.

2.5 Mechanical properties

2.5.1 Compressive strength

The compressive strengths (σ_c) of the cements were evaluated in accordance with ISO9917 [39]. Cylindrical Samples were tested after 1, 7 and 30 days. Testing was undertaken on an Instron 4082 Universal Testing Machine (Instron Ltd., High Wycombe, Bucks, UK) using a 5 kN load cell at a crosshead speed of 1 mm/min^{-1}.

2.5.2 Biaxial flexural strength

The flexural strengths (σ_f) of the cements were evaluated by a method described by Williams et al. [40]. Cement discs were tested after 1, 7 and 30 days. Testing was undertaken on an Instron 4082 Universal Testing Machine (Instron Ltd., High Wycombe, Bucks, UK) using a 1 kN load cell at a crosshead speed of 1 mm/min^{-1}.

2.6 Statistical analysis

One-way analysis of variance (ANOVA) was employed to compare the handling and mechanical properties of the Ga cements (*LGa-1* and *LGa-2*) to the control (*Lcon.*) cement and where relevant, any changes occurring with respect to PAA concentration and maturation time. Comparison of relevant means was performed using the post hoc Bonferroni test. Differences between groups were deemed significant when $P \leq 0.05$. Statistical analysis was performed using SPSS software for windows version 16 (SPSS Inc. Chicago, IL).

3 Results and discussion

This work sees the development of a series of Ga-containing GPCs. The initial focus of this study was to develop the Ga-glass (*LGa-1, LGa-2*) series and evaluate any structural differences resulting from the inclusion of Ga, when compared to a Ga-free control (*Lcon.*) glass. When developing a novel series of glasses, proper characterization of the glass phase is important in order to clarify the structural role of the added ion. In conventional GPCs for example, aluminium (Al^{3+}) partly replaces silica (Si), imparting a negative charge on the glass network. As Al^{3+} cannot form a glass by itself, it is termed a *network intermediate* as it can act as either a *network former* or *modifier*. Cations such as sodium (Na^{+}) and calcium (Ca^{2+}) in conventional GPCs can charge balance the Al in these glasses or can act as network modifiers themselves [3], disrupting the connectivity of the Si–O–Si network by introducing Non-Bridging Oxygen species (NBOs), Si–O–NBO. While the role of a number of network intermediates has been discussed in the literature [18] the role of Ga in relation to GPCs formation is relatively unknown. As Ga^{3+} has a similar valence state to Al^{3+} it may be possible that it performs a similar structural role.

Initial characterization includes X-ray Diffraction (XRD) to determine if any crystalline phases were present. Figure 1a presents XRD data and it is evident that no crystalline species were introduced in either *Lcon.*, *LGa-1* or *LGa-2* during glass forming. This is important as any subsequent changes in the properties of the materials will

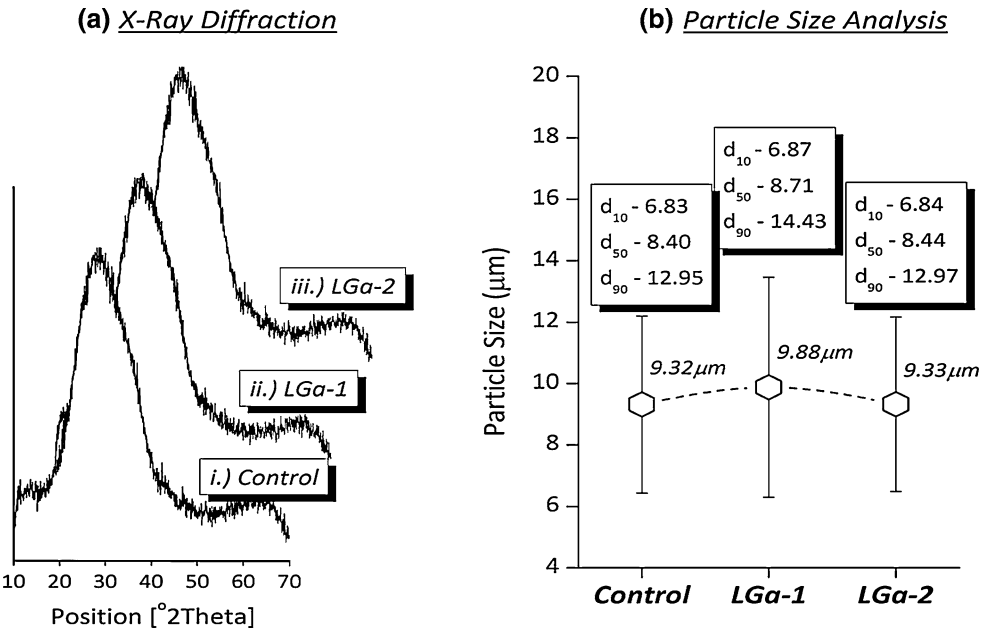

Fig. 1 **a** XRD patterns of Ga-glass series and **b** particle size analysis

be due to the intentional inclusion of Ga and not due to any phase changes in the starting glass.

Each glass was then processed in a similar fashion and subjected to Particle Size Analysis (PSA) and is presented in Fig. 1b. PSA revealed a similar mean particle size for each glass. *Lcon.* had a mean particle diameter of 9.32 µm while similar values were found for both *LGa-1* (9.88 µm) and *LGa-2* (9.33 µm). The particle distribution for each material was also similar where it ranged from approximately 6.8–13.4 µm. In relation to cement formation, particle size is important as smaller particles will dissolve more rapidly than the larger ones resulting in a quicker set. Regarding these materials, the particle size is similar so the setting reaction rate will be a result of Ga inclusion in the glass.

In formulating the glass series a theoretical calculation based on the composition of the glass was used in order to determine to role taken by Ga as acting as both a *network former* and also as a *network modifier*. The network connectivity is a calculation based on the amount of bridging oxygens (BO) in the glass, where for example a NC of two represents a silicate structure with two BOs. Figure 2a

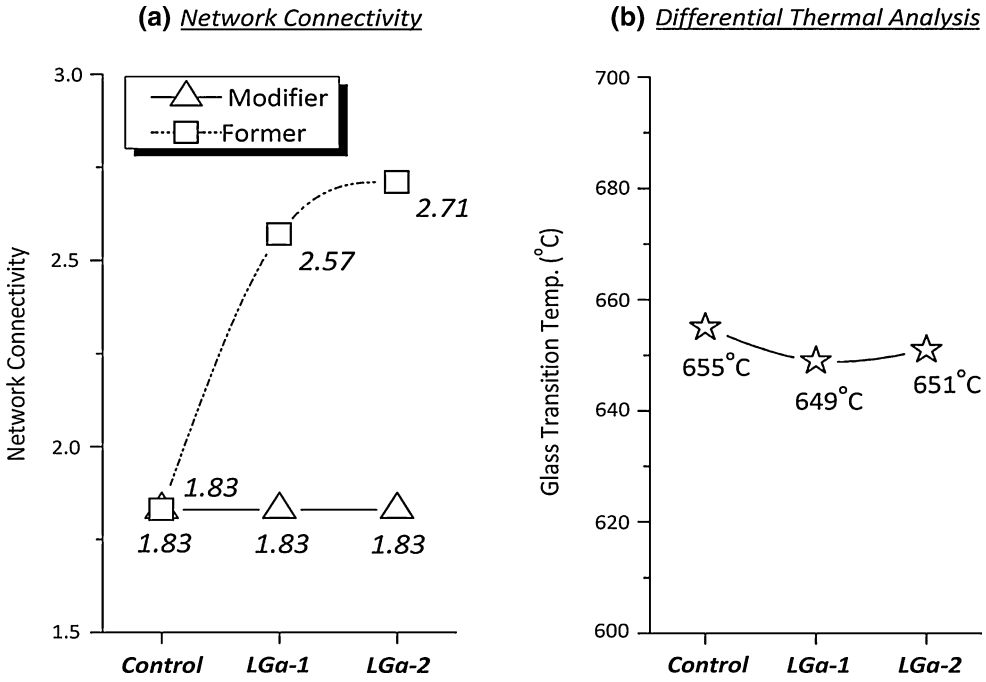

Fig. 2 **a** Glass transition temperature and **b** Network connectivity calculations

shows the NC of the glass series as both a network former and network modifier. The control glass (*Lcon.*) was calculated to have a NC of 1.83. As the Ga concentration increases to 8 mol% substituting for Zn, the NC increases when taking Ga to be a *network former*. It increases to 2.5 (*LGa-1*) and then to 2.7 (*LGa-2*) with the addition of 16 mol% Ga. When considering Ga as a *network modifier*, its substitution for Zn does not exhibit any change as its role in this instance is analogous to Zn. In this case the NC value remains at 1.83 for all materials.

Differential Thermal Analysis (DTA) was used to determine the glass transition temperature (T_g) of each glass. The T_g found for *Lcon*. was found to be 655 °C while the T_g of the Ga-containing glasses were 649 and 651 °C for *LGa-1* and *LGa-2* respectively. The change in T_g between *Lcon.* and the Ga-containing glasses is relatively insignificant (~6 °C) considering up to 16 mol% addition of Ga was present in *LGa-2*. This indicates that the Ga in this case adopts a *network modifying* role. If Ga was acting as a *network former*, a higher T_g would be expected as it would require more thermal energy the depolymerise the higher concentration of Si–O–Si species within the glass. In this case, Ga acting in the form of a network modifier is preferable as network modifiers will result in a higher concentration of non-bridging oxygens (NBOs), and these groups facilitate acid degradability and ion release during cement formation.

X-ray Photoelectron Spectroscopy was initially employed in order to confirm the composition of each of the glasses. Figure 3 shows the XPS survey scans of *Lcon.*, *LGa-1* and *LGa-2*. Figure 3a presents *Lcon.* exhibiting peaks relating to the composition of the glass. The XPS survey confirms the starting formulation of the glass whereby it was found to contain Ca_{2p3}, Zn_{2p3}, Si_{2p}, O_{1s}. Carbon (C_{1s}) was also detected as it is used in sample preparation. Figure 3a and b shows the XPS survey for *LGa-1* and *LGa-2* respectively. *LGa-1* and LGa-2 were found to contain the same elements as *Lcon.*, as expected, however with the addition of Ga_{2p3}.

High resolution XPS was also undertaken in order to determine the effect of adding Ga to the glass series. Figure 4 presents the signal for both Oxygen (O_{1s}) and Gallium (Ga_{2p3}). Regarding O_{1s}, *Lcon.* was found to have a binding energy (B.E.) of 530.5 eV. With the addition of 8 mol% Ga, there was no shift in B.E. experienced by *LGa-1*. However with the addition of 16 mol% Ga, the B.E. experienced a slight shift to 530.3 eV. This shift may be a result of the increased Ga concentration further depolymerising the silicate network, slightly increasing the concentration of NBO species [34]. Further resolution of

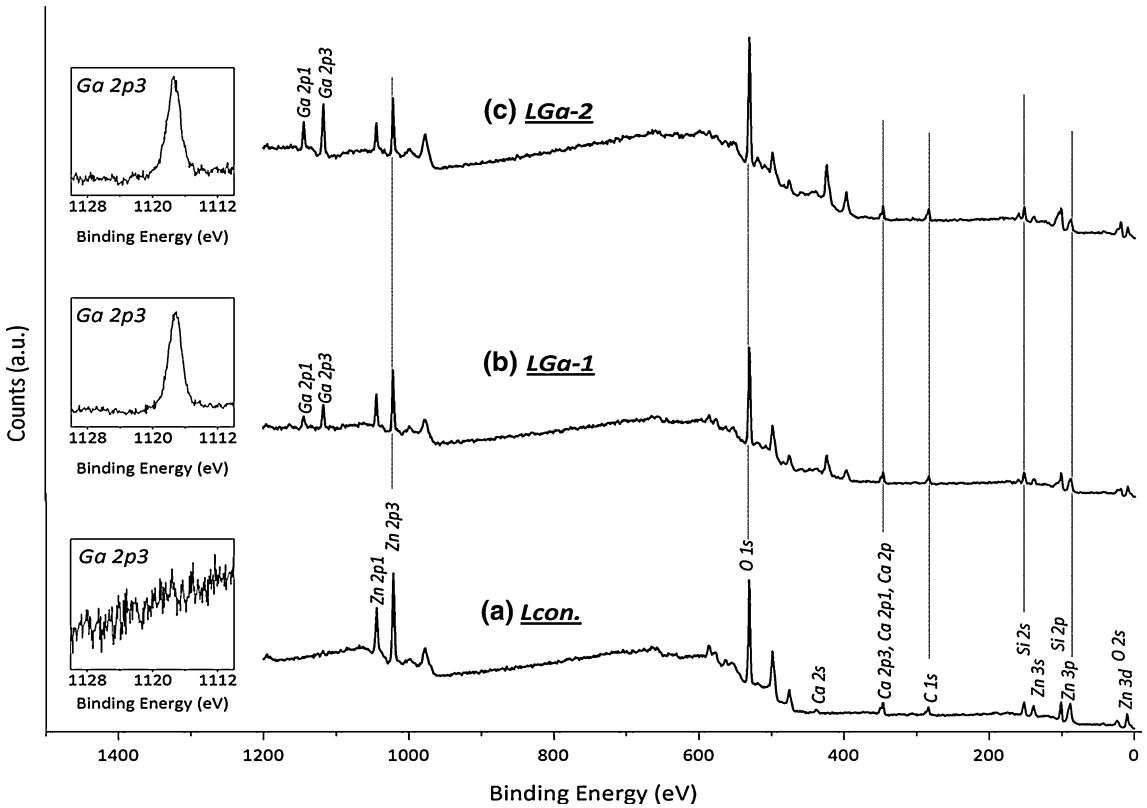

Fig. 3 XPS Survey of **a** *Lcon*, **b** *LGa-1* and **c** *LGa-2*

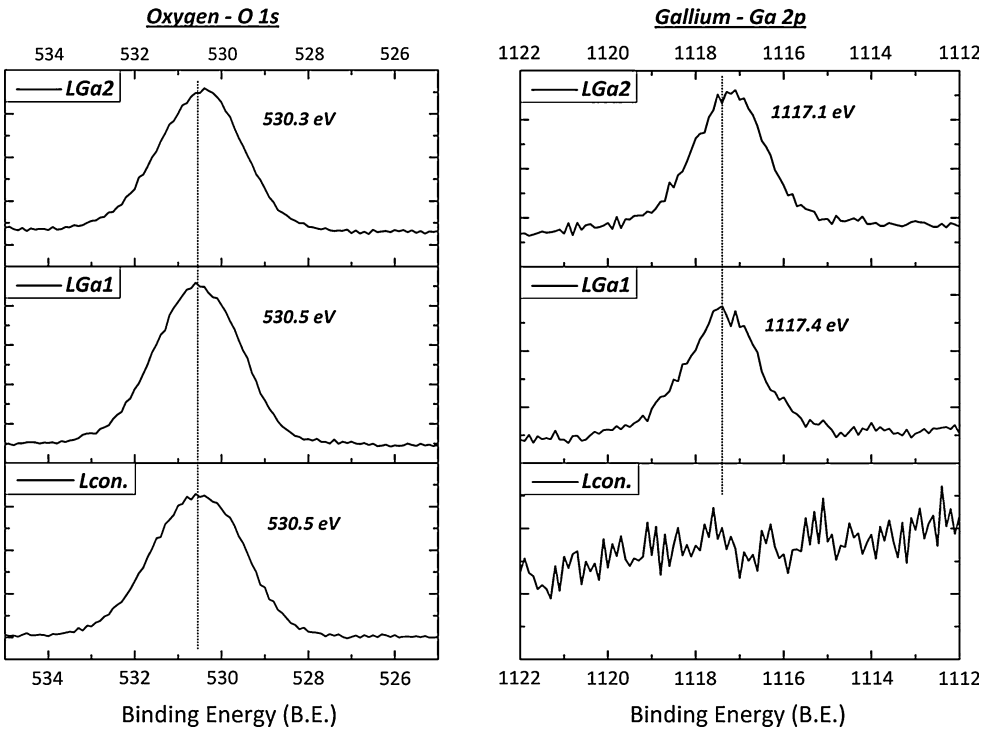

Fig. 4 High resolution XPS of oxygen (O 1 s) and gallium (Ga 2p)

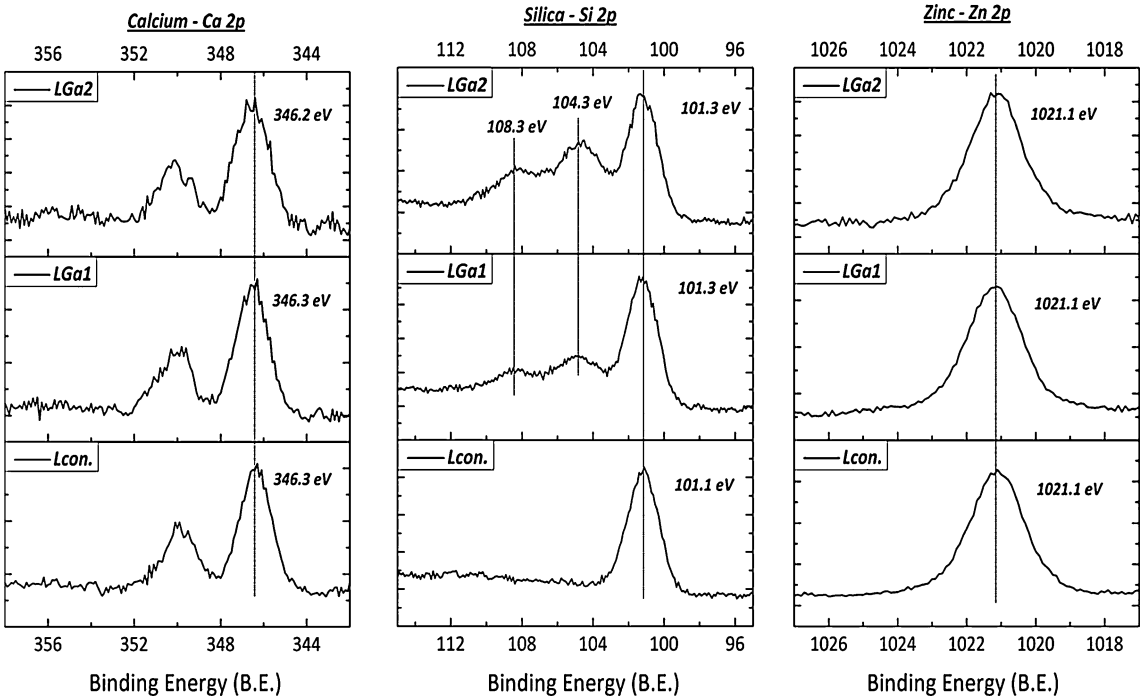

Fig. 5 High resolution XPS of calcium (Ca 2p), silica (Si 2p) and zinc (Zn 2p)

the O1s signal in each case would be required in order to confirm this. This result however, agrees with NC calculations and the relatively little change T_g where Ga addition to the glass adopts a network modifying role. Figure 4 also presents the peak for Ga which is present at 1117.4 eV (*LGa-1*) and 1117.1 eV (*LGa-2*), however the slight shift in this case may be due to the noise of the signal.

High resolution scans were also performed on Calcium (Ca_{2p}) Silica (Si_{2p}) and Zinc (Zn_{2p}) and are presented in Fig. 5. There was found to be no significant shift in the

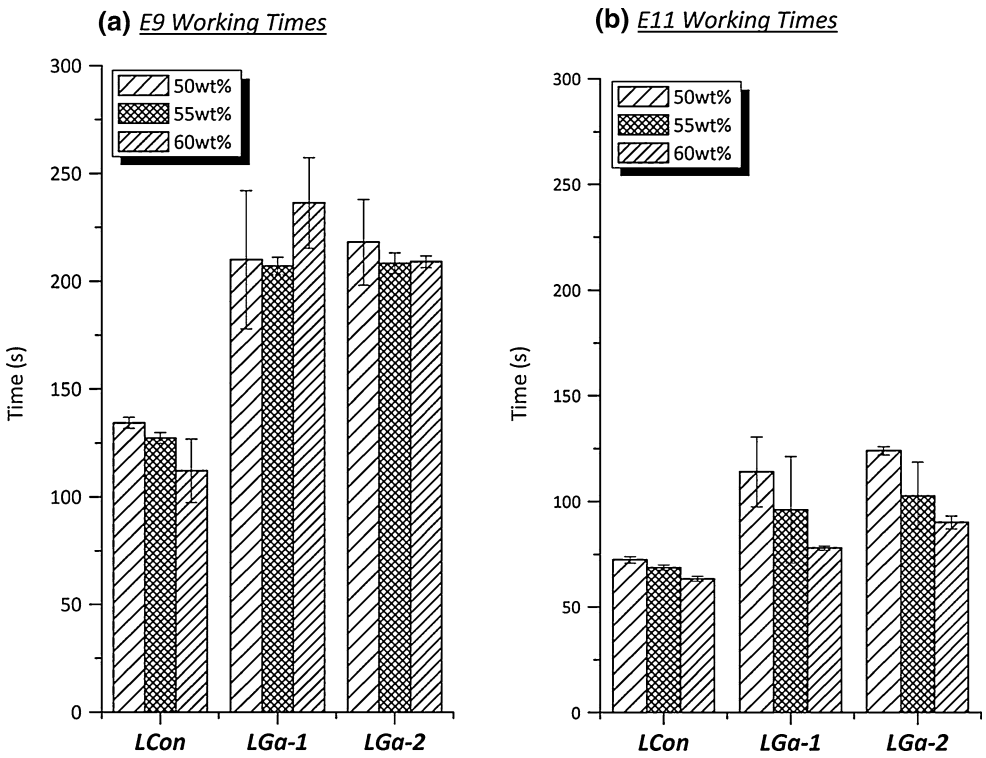

Fig. 6 Working times of E9 and E11 PAA cement series

Ca_{2p} peak with the addition of Ga in the glass series, the peak was identified at 346.3 eV (*Lcon.*), 346.3 eV (*LGa-1*) and 346.2 eV (*LGa-2*). However the Si_{2p} did experience a different signal when Ga was added to the glass. Although the actual peak position was the same for each glass (*Lcon.*, *LGa-1* and *LGa-2*) at 101.3 eV. However satellite peaks were identified with increasing intensity with increasing Ga concentration at approximately 104.9 and 108.4 eV for both *LGa-1* and *LGa-2* respectively. This is likely due to Ga overlapping the Si signal at a lower B.E. due to it being in a different electronic configuration. In the case of the peak at 104.3 eV the peak is likely attributed to $Ga_{3p3/2}$ which overlaps at this B.E. [41]. The peak present at 108.4 eV may be attributed $Ga_{3p1/2}$ whereas the main peak at 101.3 eV is Si–O–Si groups [42]. High resolution spectra found for Zn was determined at the same B.E. (1021.1 eV) also for each glass.

Ga-containing GPCs were formulated as described in "Materials and methods" section, with PAAs with different molecular weight (E9 and E11). For this section the acid component was added also at different concentrations (50, 55 and 60 wt%) to determine any increase/decrease relating to the acid chain length. Figure 6a presents the working time (T_w) of the cement series using E9 PAA. From Fig. 6a it can be seen that there is a decrease in the T_w as the concentration of PAA increases in *Lcon.* The T_w decreases from 134 to 112 s when increasing the PAA from 50 to 60 wt%, which is expected as with an increase in the concentration of $COOH^-$ groups, there is a subsequent increase in the rate of gelation. *LGa-1* and *LGa-2* experienced similar T_w with E9 ranging from approximately 210–240 s for both cements, however there was no significant change with respect to PAA concentration. When comparing cements at the same PAA concentration (i.e., 50, 55, 60 wt%) it was found that there was a significant increase in each case when comparing both Ga-cements (*LGa-1* and *LGa-2*) to the control cement (*Lcon.*) where *p* values ranged from $P = 0.000$–0.016 (Table 2). However there was no significant difference determined between *LGa-1* and *LGa-2* ($P = 0.199$–1.000). Regarding E11 PAA, as was expected the cements experienced a much shorter T_w. *Lcon.* exhibited the shortest T_w which reduced from 72 to 63 s as the PAA concentration increased from 50 to 60 wt%. Both *LGa-1* and *LGa-2* experienced a similar trend in this instance, where *LGa-1* decreased from 114 to 78 s and *LGa-2* decreased from 124 to 90 s with the increase in PAA concentration. There was

Table 2 Working time statistics (significant at $*P = 0.05$)

		50 wt%	55 wt%	60 wt%
E9 PAA	Lcon. v. LGa-1	0.016*	0.000*	0.000*
	Lcon. v. LGa-2	0.010*	0.000*	0.001*
	LGa-1 v. LGa-2	1.000	1.000	0.199
E11 PAA	Lcon. v. LGa-1	0.014*	0.014*	0.000*
	Lcon. v. LGa-2	0.010*	0.010*	0.000*
	LGa-1 v. LGa-2	1.000	1.000	0.001*

also found to be a significant increase in T_w when comparing *Lcon.* to *LGa-1* and *LGa-2* at 50, 55 and 60 wt% PAA additions ($P = 0.000$–0.014). There was no significant difference between *LGa-1* and *LGa-2* at 50 wt% ($P = 1.000$) and 55 wt% ($P = 0.000$), however at 60 wt% ($P = 0.001$) a significant difference was determined (Table 2).

The setting times (T_s) in each case were completed in accordance with the ISO standard for dental water based materials. The T_s experienced a similar trend to the T_w, where the Ga-containing cements (*LGa-1* and *LGa-2*) experienced much longer T_s than the control (*Lcon.*) regardless of the PAA (E9 or E11). Considering E9, both *LGa-1* and *LGa-2* had similar T_s at 50 and 60 wt% PAA additions where the T_s were approximately 560 s (9.3 min). *LGa-1* and *LGa-2* also had similar T_s at 60 wt% E9, where the T_s were found to be approximately 774 s (13 min). T_s within this region are generally considered too long for applications in orthopaedics as open exposure during cement setting can leave patients vulnerable to septic complications [43]. When comparing *Lcon.* to *LGa-1* and *LGa-2* at 50, 55 and 60 wt% PAA, there was a significant increase in T_s in each case ($P = 0.000$). There was no significant change when comparing *LGa-1* and *LGa-2* ($P = 0.057$–1.000, Table 3) at each PAA concentration (Fig. 7).

Cements formulated with E11 PAA experienced shorter T_s than cements formulated with E9, as was expected. *Lcon.* cements were found to have similar T_s of approximately 104 s regardless of PAA concentration. Both *LGa-1* and *LGa-2* had T_s ranging from 197 to 232 s, and the concentration of PAA used did not show and significant change. When comparing *Lcon.* to both *LGa-1* ($P = 0.000$) and *LGa-2* ($P = 0.000$), there was a significant increase with each concentration of PAA (50, 55, 60 wt%). When comparing *LGa-1* and *LGa-2*, no significant change occurred with 50 and 55 wt% PAA additions, however with 60 wt% PAA a slight change was observed (Table 3). From rheological testing it is evident that the addition of Ga increases the T_w and T_s, however the concentration of PAA and the mol% of Ga in the starting glass (0.08 or 0.016 mol%) does not seem to influence the setting. The increase in rheology can be attributed to the presence of Ga^{3+} within the starting glass, and may influence the setting by causing a higher level of disruption by either disrupting Ca^{2+}–COO^{-} formation or neutralizing the pH of the cement matrix thus retarding the setting process,

Table 3 Setting time statistics (significant at $*P = 0.05$)

		50 wt%	55 wt%	60 wt%
E9 PAA	Lcon. v. LGa-1	0.000*	0.000*	0.000*
	Lcon. v. LGa-2	0.000*	0.000*	0.000*
	LGa-1 v. LGa-2	0.819	0.057	1.000
E11 PAA	Lcon. v. LGa-1	0.000*	0.000*	0.000*
	Lcon. v. LGa-2	0.000*	0.000*	0.000*
	LGa-1 v. LGa-2	1.000	1.000	0.002*

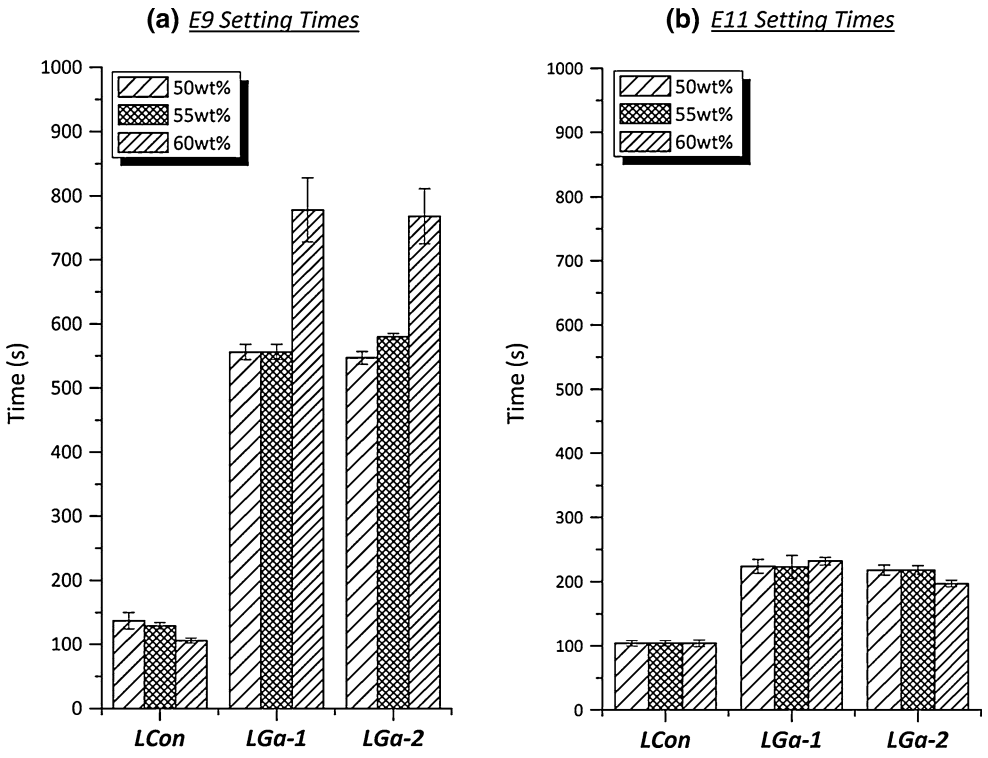

Fig. 7 Setting times of E9 and E11 PAA cement series

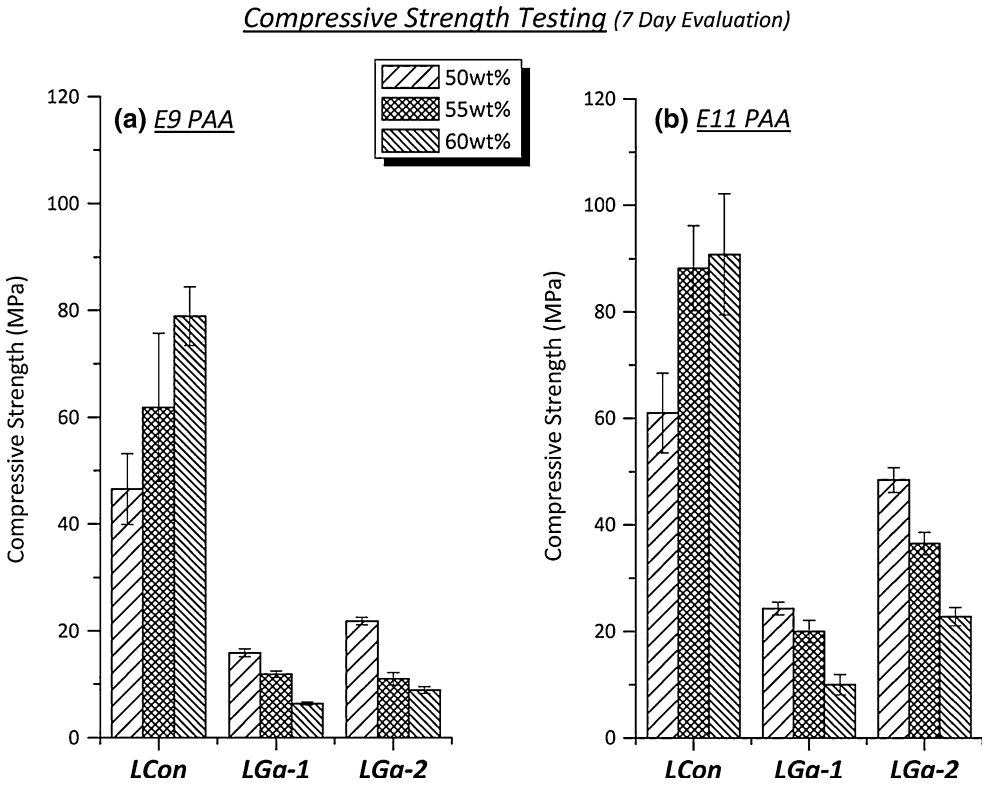

Fig. 8 Compressive strength of each E9 and E11 cement formulation after 7 days

however further studies will be required to confirm the precise role that Ga plays in GPC formation.

Compressive testing (σ_c) was undertaken after 7 days for each cement formulation with E9 and E11 PAA at 50, 55 and 60 wt% concentrations in order to determine the effect that PAA molecular weight and PAA concentration has on the mechanical strength. Figure 8a presents the σ_c regarding the E9 PAA cement series. It is evident with the *Lcon.* cement that there is a significant increase in σ_c (46–78 MPa, $P = 0.017$) as the PAA concentration increases from 50 to 60 wt%. However, the Ga-containing cements *LGa-1* and *LGa-2* had a much lower mean σ_c than *Lcon.*, and it was found with these cements that the σ_c decreased from 15 to 6 MPa ($P = 0.000$) for *LGa-1* and from 22 to 9 MPa ($P = 0.000$) for *LGa-2*.

A similar trend was observed with the E11 cements and is presented in Fig. 8b. *Lcon.* increased in strength from 61 to 80 MPa ($P = 0.003$). LGa-1 experienced a significant decrease in σ_c from 24 to 12 MPa ($P = 0.000$), and *LGa-2* decreased in σ_c from 48 to 22 MPa ($P = 0.000$). This is likely due to Ga^{3+} disrupting polyacrylate formation during the setting reaction, as it is known that Ca^{2+}–COO^- and Zn^{2+}–COO^- bonding on the acid chains are responsible for cement setting [18]. The *Lcon.* cements act as expected where the increase in PAA concentration results in a higher mechanical strength due to the higher concentration of COO^- groups available for forming ionic crossbridges within the cement matrix. The Ga-cements were found to reduce in strength as the PAA concentration increases, which may be a consequence of pH imbalance between the PAA concentrations and the Ga-glasses, however a full IR study would be required in order to fully determine the role of Ga^{3+} in these cements.

The cement formulation with the more suitable handling and mechanical properties were selected for further testing (i.e., E11 PAA with 50 wt% concentration). Each cement was tested for compressive (σ_c) and biaxial flexural strength (σ_f) over 1, 7 and 30 days incubated at 37 °C. *Lcon.* σ_c increased from 62 to 68 MPa over 1–30 days, however this increase did not reach significance. *LGa-1* significantly increased in σ_c from 14 to 42 MPa ($P = 0.000$), and *LGa-2* increased in σ_c from 20 to 47 MPa ($P = 0.000$). Similar observations were made with σ_f testing where *Lcon.* increased in σ_f from 29 to 42 MPa ($P = 0.020$), *LGa-1* from 7 to 32 MPa ($P = 0.000$) and *LGa-2* from 12 to 36 MPa ($P = 0.000$). The increase in both σ_c and σ_f is likely due to the dissolution of the glass particles with respect to maturation. Dissolution of the glass particles within the cement results in the release of ions that further crosslink PAA chains within the cement matrix [18] (Fig. 9).

For this work a Ga-containing glass series was initially developed and characterized. Ga-cements were developed with suitable handling and mechanical properties for use as therapeutic bone cements. Further spectroscopic studies will need to be done in order to fully understand the role of

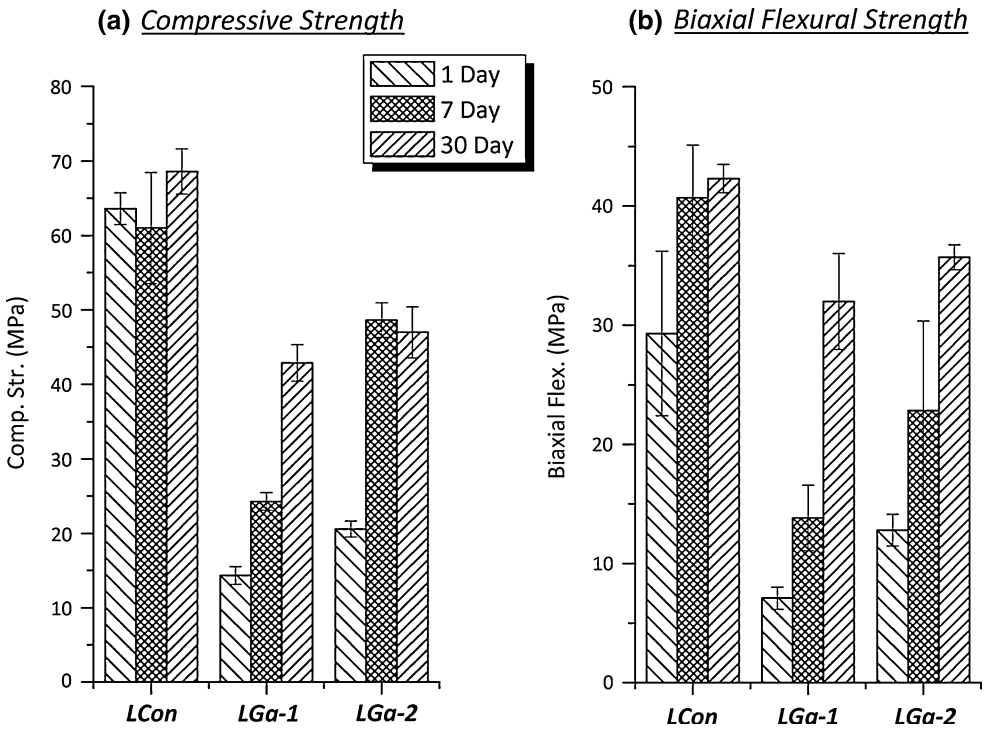

Fig. 9 **a** Compressive and **b** biaxial flexural strength of E11 +50 wt% over 1, 7 and 30 days

Ga^{3+} regarding GPC setting and maturation. Ion release and cell culture studies will also need to be completed in order to determine the concentrations and therapeutic effect of Ga release from these cements.

References

1. Hench L, Peitl O, Zanotto ED. Highly bioactive P_2O_5–Na_2O–CaO–SiO_2 glass ceramics. J Non Cryst Sol. 2001;292:115–26.
2. Hench LL. The story of bioglass. J Mater Sci Mater Med. 2006; 17:967–78.
3. Kokubo T, Takadama H. How useful is SBF in predicting in vivo bone bioactivity. Biomaterials. 2006;27:2907–15.
4. Kokubo T, Kim H-M, Kawashita M. Novel bioactive materials with different mechanical properties. Biomaterials. 2003;24: 2161–75.
5. Heikkilä JT, Aho AJ, Kangasniemi I, Yli-Urpo A. Polymethylmethacrylate composites: disturbed bone formation at the surface of bioactive glass and hydroxyapatite. Biomaterials. 1996;17(18): 1755–60.
6. Daglilar S, Erkan ME, Gunduz O, Ozyegin LS, Salman S, Agathopoulos S, Oktar FN. Water resistance of bone-cements reinforced with bioceramics. Mater Lett. 2007;61(11–12): 2295–8.
7. Lacefield WR, Hench LL. The bonding of Bioglass® to a cobalt-chromium surgical implant alloy. Biomaterials. 1986;7(2):104–8.
8. Fu Q, Rahaman MN, Sonny Bal B, Brown RF, Day DE. Mechanical and in vitro performance of 13–93 bioactive glass scaffolds prepared by a polymer foam replication technique. Acta Biomater. 2008;4(6):1854–64.
9. Rezwan K, Chen QZ, Blaker JJ, Boccaccini AR. Biodegradable and bioactive porous polymer/inorganic composite scaffolds for bone tissue engineering. Biomaterials. 2006;27(18):3413–31.
10. Boccaccini AR, Blaker JJ, Maquet V, Day RM, Jérôme R. Preparation and characterisation of poly(lactide-co-glycolide) (PLGA) and PLGA/Bioglass® composite tubular foam scaffolds for tissue engineering applications. Mater Sci Eng, C. 2005;25: 123–31.
11. Brown RF, Day DE, Day TE, Jung S, Rahaman MN, Fu Q. Growth and differentiation of osteoblastic cells on 13–93 bioactive glass fibers and scaffolds. Acta Biomater. 2008;4(2):387–96.
12. Cannillo V, Chiellini F, Fabbri P, Sola A. Production of Bioglass® 45S5-Polycaprolactone composite scaffolds via salt-leaching. Compos Struct. 2010;92(8):1823–32.
13. Chen QZ, Thompson ID, Boccaccini AR. 45S5 Bioglass®-derived glass-ceramic scaffolds for bone tissue engineering. Biomaterials. 2006;27(11):2414–25.
14. Chen Q-Z, Rezwan K, Françon V, Armitage D, Nazhat SN, Jones FH, Boccaccini AR. Surface functionalization of Bioglass®-derived porous scaffolds. Acta Biomater. 2007;3(4):551–62.
15. Jones JR, Ehrenfried LM, Hench LL. Optimising bioactive glass scaffolds for bone tissue engineering. Biomaterials. 2006;27: 7964–73.
16. Vargas GE, Mesones RV, Bretcanu O, López JMP, Boccaccini AR, Gorustovich A. Biocompatibility and bone mineralization potential of 45S5 Bioglass®-derived glass-ceramic scaffolds in chick embryos. Acta Biomater. 2009;5(1):374–80.
17. Hatton PV, Hurrell-Gillingham K, Brook IM. Biocompatability of glass ionomer bone cements. J Dent. 2006;34:598–601.
18. Nicholson JW, Wilson AD. Chemistry of solid state materials Vol 3: acid–base cements—their biomedical and industrial applications. Cambridge: Cambridge University; 1993.
19. Billington RW, Williams JA, Pearson GJ. Ion processes in glass ionomer cements. J Dent. 2006;34:544–55.
20. Carter DH, Sloan P, Brook IM, Hatton PV. Role of exchanged ions in the integration of ionomeric (glass polyalkenoate) bone substitutes. Biomaterials. 1997;18:459–66.
21. Van Duinen RNB, Kleverlaan CJ, de Gee AJ, Werner A, Feilzer AJ. Early and long-term wear of 'Fast-set' conventional glass–ionomer cements. Dent Mater. 2005;21(8):716–20.

22. Cho S, Cheng AC. A review of glass ionomer restorations in the primary dentition. J Can Dent Assoc. 1999;65:491–5.
23. Smith DC. Development of glass–ionomer cement systems. Biomaterials. 1998;19:6467–78.
24. Tyas MJ, Burrow MF. Adhesive restorative materials: a review. Aust Dent J. 2004;49(3):112–21.
25. DeBruyne MAA, DeMoor RJG. The use of glass ionomer cements in both conventional and surgical endodontics. Int Endo J. 2004;37:91–104.
26. Firling CE, Hill TA, Severson AR. Aluminium toxicity perturbs long bone calcification in the embryonic chick. Arch Toxicol. 1999;73:359–66.
27. Hoang-Xuan K, Perrotte P, Dubas F, Philippon J, Poisson FM. Myoclonic encephalopathy after exposure to aluminium. Lancet. 1996;347:910–1.
28. Reusche E, Pilz P, Oberascher G, Linder B, Egensperger R, Gloeckner K, Trinka E, Iglseder B. Subacute fatal aluminium encephalopathy after reconstructive otoneurosurgery: a case report. Hum Pathol. 2001;32(10):1136–9.
29. Boyd D, Clarkin OM, Wren AW, Towler MR. Zinc-based glass polyalkenoate cements with improved setting times and mechanical properties. Acta Biomater. 2008;4(2):425–31.
30. Boyd D, Towler MR. The processing, mechanical properties and bioactivity of zinc based glass ionomer cements. J Mater Sci Mater Med. 2005;16:843–50.
31. Boyd D, Towler MR, Watts S, Hill R, Wren AW, Clarkin OM. The role of Sr^{2+} on the structure and reactivity of SrO–CaO–ZnO–SiO_2 ionomer glasses. J Mater Sci Mater Med. 2008;19:953–7.
32. Boyd D, Towler MR, Wren AW, Clarkin OM. Comparison of an experimental bone cement with surgical simplex p, spineplex and cortoss. J Mater Sci Mater Med. 2007;19(4):1745–52.
33. Wren AW, Kidari A, Cummins NM, Towler MR. A spectroscopic investigation into the setting and mechanical properties of titanium containing glass ionomer cements. J Mater Sci Mater Med. 2010;21:2355–64.
34. Wren AW, Laffir FR, Kidari A, Towler MR. The structural role of titanium in Ca–Sr–Zn–Si/Ti glasses for medical applications. J Non Cryst Sol. 2010;357:1021–6.
35. Wren AW, Cummins NM, Laffir FR, Hudson SP, Towler MR. The bioactivity and ion release of titanium-containing glass polyalkenoate cements for medical applications. J Mater Sci Mater Med. 2011;22:19–28.
36. Ortega R, Suda A, Devès G. Nuclear microprobe imaging of gallium nitrate in cancer cells. Nucl Instrum Methods Phys Res Sect B Beam Inter Mater Atoms. 2003;210:364–7.
37. Chitambar CR. Medical applications and toxicities of gallium compounds. Int J Environ Res Public Health. 2010;7(52):337–61.
38. Collery P, Keppler B, Madoulet C, Desoize B. Gallium in cancer treatment. Crit Rev Oncol Hematol. 2002;42(3):283–96.
39. International Organization for Standardization 9917. Dental water based cements (E), in Case Postale 56. 1991: Geneva, Switzerland. p. CH-11211.
40. Williams JA, Billington RW, Pearson GJ. The effect of the disc support system on biaxial tensile strength of a glass ionomer cement. Dent Mater. 2002;18(5):376–9.
41. Romand M, Roubin M, Deloume J-P. X-ray photoelectron emission studies of mixed selenides AgGaSe2 and Ag9GaSe6. J Sol State Chem. 1978;25:159–64.
42. Gray RC, Carver JC, Hercules DM. An ESCA study of organo-silicon compounds. J Elec Spec Rel Phen. 1976;8:5343–57.
43. Bahna P, Dvorak T, Hanna H, Yasko AW, Hachem R, Raad I. Orthopaedic metal devices coated with a novel antiseptic dye for the prevention of bacterial infection. Int J Anti Agents. 2007;29:593–6.